Supporting Information

Engineering 3D parallelized microfluidic droplet generators with equal flow profiles by computational fluid dynamics and stereolithographic printing

Tom Kamperman, [‡] *Liliana Moreira Teixeira,* [‡] *Seyedeh Sarah Salehi,* [‡] *Greet Kerckhofs, Yann Guyot, Mike Geven, Liesbet Geris, Dirk Grijpma, Sebastien Blanquer, and Jeroen Leijten* *

[‡] Co-first authors who contributed equally to this work. Author sequence was randomly determined.

* Correspondence: Dr. Jeroen Leijten (email: jeroen.leijten@utwente.nl)

Keywords: 3D printing; stereolithography; droplet microfluidics; microgels; 3D cell culture

1

Experimental Section

Materials: PIC100 resin was purchased from EnvisionTec. HRP (type VI), hydrogen peroxide, hexadecane oil, fetal bovine serum (FBS), ascorbic acid, iodixanol (Optiprep), glutamax, Penicillin and Streptomycin (100 U/ml, 100 μg/ml), and trypsin-EDTA, Span 80, calcein AM, ethidium homodimer-1 (EthD-1), and fluorescein were purchased from Sigma-Aldrich. Minimal essential medium α with nucleosides (α-MEM) was purchased from Gibco. Phosphate-buffered saline (PBS) was purchased from Lonza. Basic fibroblast growth factor (ISOKine bFGF) was purchased from Neuromics. Gastight syringes (Hamilton), tubing and connectors were purchased from IDEX Health and Science. Low-pressure syringe pumps (neMESYS) were purchased from Cetoni. Silicone tubing (510 μm ID, 940 μm OD) was purchased from Helix Medical. Dex-TA (~16 g/mol, DS ~15) was synthesized as previously described.[1] Human bone marrow-derived mesenchymal stem cells (MSCs) were isolated from fresh bone marrow samples and cultured as previously described.[2] The use of patient materials was approved by the local ethical committee of the Medisch Spectrum Twente and informed written consent was obtained for all samples.

3D printing of microfluidic droplet generators: 3D printed microfluidic droplet generators were designed using CAD software of Rhinoceros3D (McNeel, Europe). Microdevice fabrication was performed using a commercially available stereolithography printer (EnvisionTec Perfactory 3 Mini Multi Lens), equipped with a digital micromirror device allowing projections of 1280×1024 pixels, each measuring 32×32 μm^2. The microdevices were built using a layer-by-layer method, with a maximal single layer thickness of 50 μm and sequential exposure photo-curing of 9 s. Light intensity was fixed at 180 mW/dm^2 and the wavelength of the blue light irradiation ranged from 400 to 550 nm, with a peak at 440 nm. Commercial acrylic resin EnvisionTec PIC100 was used to fabricate all microfluidic devices. Inter-layer horizontal alignment was determined by visual analysis using ImageJ. The printed

2

microdevices were ready for use after removal of the non-crosslinked resin, which was achieved by flushing the channels with isopropanol.

Computational fluid dynamics simulations: The computational fluid dynamics simulations have been performed by solving the steady state Navier-Stokes equations with a gravity term using the solver Freefem++.[3] These equations were solved for different geometries using appropriately fine meshes for each geometry, in order to select an optimal design for the tank, spacer, outlet and inlet placing **(Figure S2)**. The manual optimization process used an optimization criterium that was based on the distribution of the incoming flow rate Q_{in} into the three outlet flow rates Q_{out_i} (i = 1,2,3), with an arbitrarily chosen acceptable value of 3% for the threshold of the difference between $Q_{in}/3$ and Q_{out_i}.

µCT image acquisition, 3D visualization, and CAD-to-µCT matching: For µCT image acquisition of all chips, a Phoenix NanoTom S (GE Measurement and Control Solutions) with a 180 kV, 15 W high-performance microfocus X-ray tube was used. An operation voltage of 50 kV and current of 190 µA was used in a filter-free manner. An exposure time of 500 ms was applied with a frame averaging of 1 and an image skip of 0 (i.e., fast scanning mode), resulting in a scanning time of 20 minutes per chip. The applied isotropic voxel size was 7-8 µm for the rectangular chips and 12.5 µm for circular chips. Prior to 3D visualization, the datasets were denoised (3D despeckling of white and black speckles below 100 voxels) and binarized, for the material or for the pore space, using Otsu segmentation (CTAn, Bruker µCT). Mimics (Materialise) was used for 3D rendering, as well as to generate STL-files of all the datasets. In order to calculate the deviation between the design and the produced parts, we matched the CAD design with the STL-files of the µCT datasets using VGSTUDIO MAX (Volume Graphics GmbH).

Cell isolation and expansion: MSCs were cultured in proliferation culture medium consisting of 10% (v/v) FBS, 1% (v/v) glutamax, 1% (w/v) AsAP, 1% (v/v) Penicillin and Streptomycin,

and 1 ng/ml bFGF (freshly added to the culture medium) in α-MEM. Prior to cell encapsulation, cells were expanded in tissue culture flasks at an initial seeding density of 3.000 cells/cm^2 in humidified incubator under 5% CO_2 at 37 °C. Culture medium was changed every 3-4 days and cells were used at passage four and at a concentration of 4×10^7 cells/ml.

Preparation of microdroplet and microgels: To produce water-in-oil droplets, water with fluorescein was emulsified in hexadecane with 1% (w/v) Span 80 at a typical total (water + oil) flow rate 200 µl/min per droplet generator. To produce solid Dex-TA microgels, 5% (w/v) Dex-TA and 22 U/ml HRP in PBS was emulsified in hexadecane with 1% (w/v) Span 80 using a microfluidic droplet generator connected to a silicone tubing. The silicone tubing was submerged in 30% (w/w) H_2O_2, which diffused through the silicone and the oil phase into the Dex-TA precursor microemulsion, thereby inducing the enzymatic crosslinking of the tyramine-conjugated polymer to yield Dex-TA microspheres, as previously described.[4] To produce Dex-TA microcapsules, the protocol for solid Dex-TA microgel production was used, but with reduced H_2O_2 supplementation, in order to maintain non-crosslinked cores. To prepare cell-laden microcapsules, also prepolymer consisting of 5% (w/v) Dex-TA in PBS and 22 U/ml HRP was used. Prior to encapsulation, cells were filtered through a 40 µm cell strainer to remove clumps and mixed with the hydrogel precursor. 8% (v/v) Optiprep was added to adjust the solution's relative density to 1.04 to avoid gravitational cell deposition. A syringe was used to load cell-laden hydrogel precursor solution and was agitated every five minutes using a magnetic micro stirring bar. Droplets were formed at the interface of the precursor solution and oil phase, with flow rate ratio of 50:1 respectively. Emulsions were broken by washing three times with hexadecane and one time with culture medium. Microgels then were maintained in standard well plates.

Cell staining and visualization: Cell viability two hours post encapsulation was assessed using a live/dead assay (Calcein-AM and EthD-1), according to manufacturer's protocol

4

(Thermofisher). Specimen were visualized using fluorescence microscopy (Nikon) and analyzed with ImageJ software. Post encapsulation metabolic activity was assessed with Presto Blue assay (Invitrogen) after 1,7,14, and 21 days of culture. Samples were analyzed after 10 minutes of incubation under 5% CO_2 at 37 ºC. Absorbance was quantified using with an automatic plate reader (Victor X3, ex. 545/10 nm, em. 590/10 nm).

Data representation and statistics: Inter-layer horizontal alignment error was measured of 35 printed layers and reported as the average ± standard deviation. Channel width measurements as a function of pressure were performed on at least three samples per condition and reported as the average ± standard deviation. Size distribution measurements of droplets were performed on at least 100 droplets per condition and plotted as histograms plus the coefficient of variation (CV = standard deviation / average). Flow throughs of parallelized microfluidic channels were measured at least three times and reported as the average ± standard deviation. Significant differences ($p < 0.05$) were concluded from one-way ANOVA tests. Metabolic activity measurements were performed on at least three samples per time point and reported as the average ± standard deviation.

Overexposed   Not overexposed
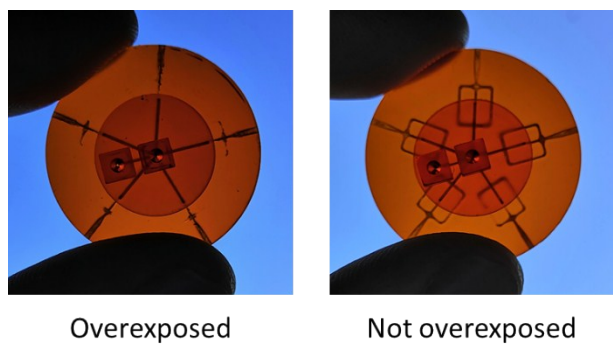
Fig. S1. Overexposure of the PIC100 resin reduced the printing resolution, causing closure of the microfluidic channels. Exposing for 9 s using a 180 mW/dm^2 projector brightness resulted in open microfluidic channels.
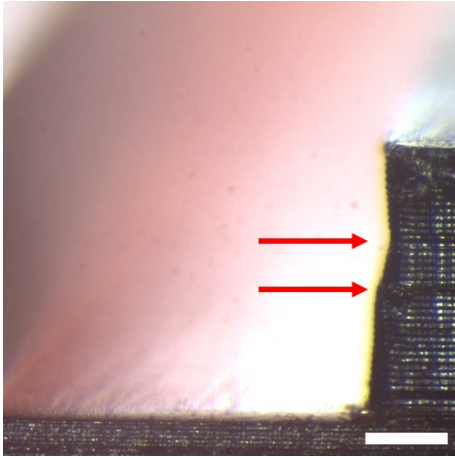
Fig. S2. Small vibrations of the work bench during printing resulted in significant inter-layer displacements, as indicated with red arrows. Scale bar indicates 250 µm.
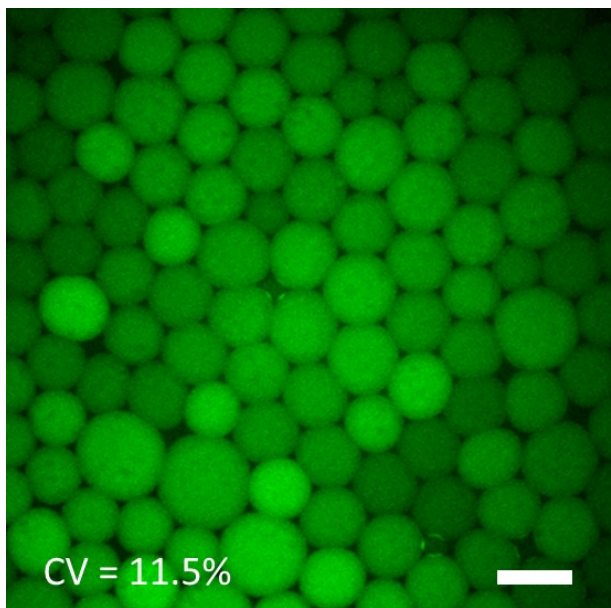
Fig. S3. The relatively rough microfluidic channel surfaces that appeared after overcuring associated with aqueous channel wetting, which led to uncontrolled droplet pinch-off and thus more polydisperse water-in-oil droplet size distributions. Scale bar indicates 500 μm.

Fig. S4. An array of individual microfluidic droplet generators fabricated in a single stereolithographic printing procedure.
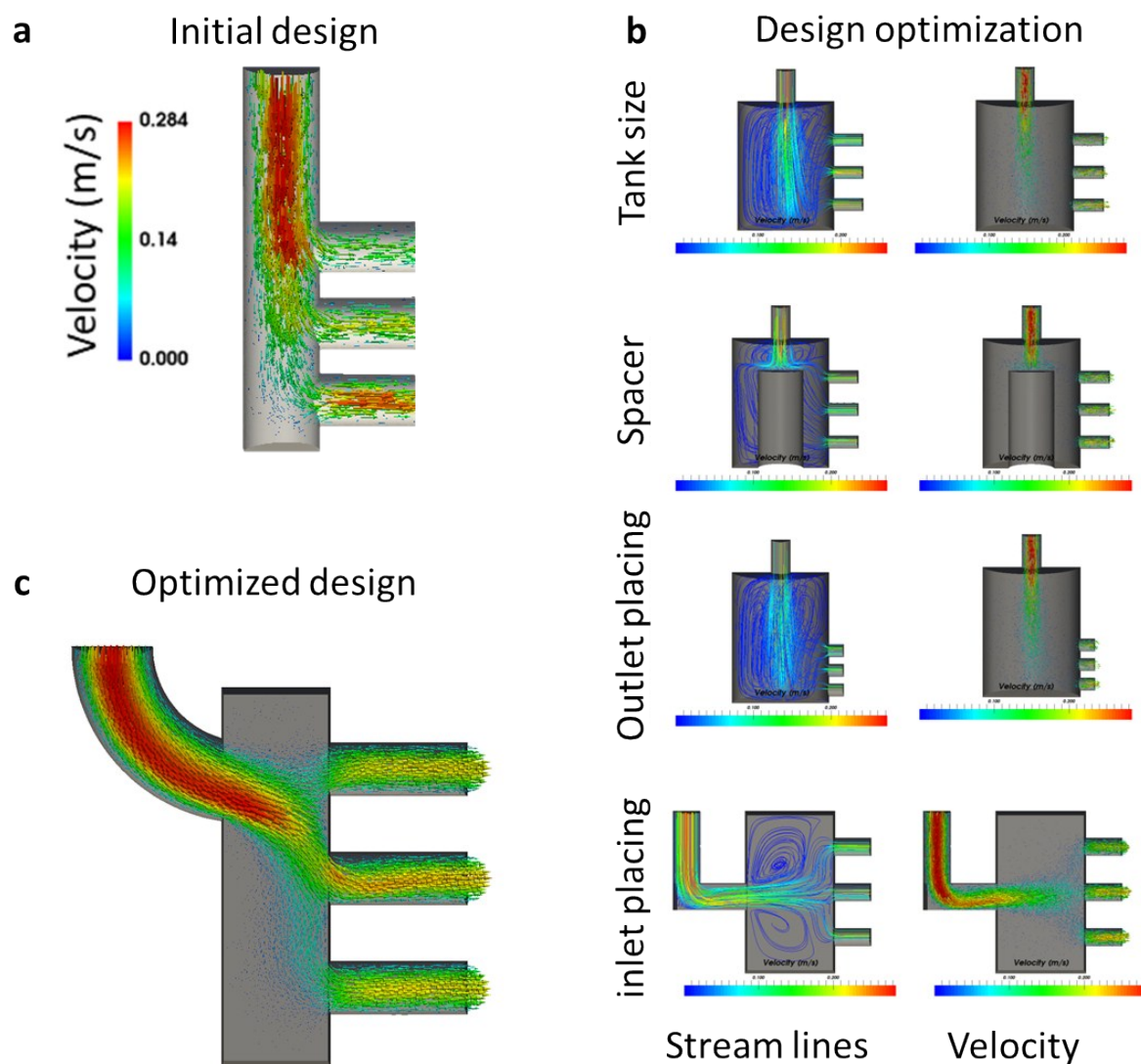
Fig S5. Computational fluid dynamics simulations of microflow distributors connected to three stacked microfluidic channels. (a-c) Various design iterations were done to come from the initial to the optimized microflow distributor design, which eventually resulted in equally distributed flow rates through all the stacked channels. First, the tank size was increased allowing the flow to decelerate, potentially resulting in more equally distributed flow over the outlets. Adding an obstacle in the tank was hypothesized to be more efficient for decelerating the flow. The outlets were put closer to further minimize flow gradients. However, best results were obtained by utilizing a 'horizontal' inflow within a smaller tank. The inlet channel was curved to avoid flow break due to a 90° turn. Finally, the inlet location was found to be the most important parameter to achieve equal flow distribution across all outlets.
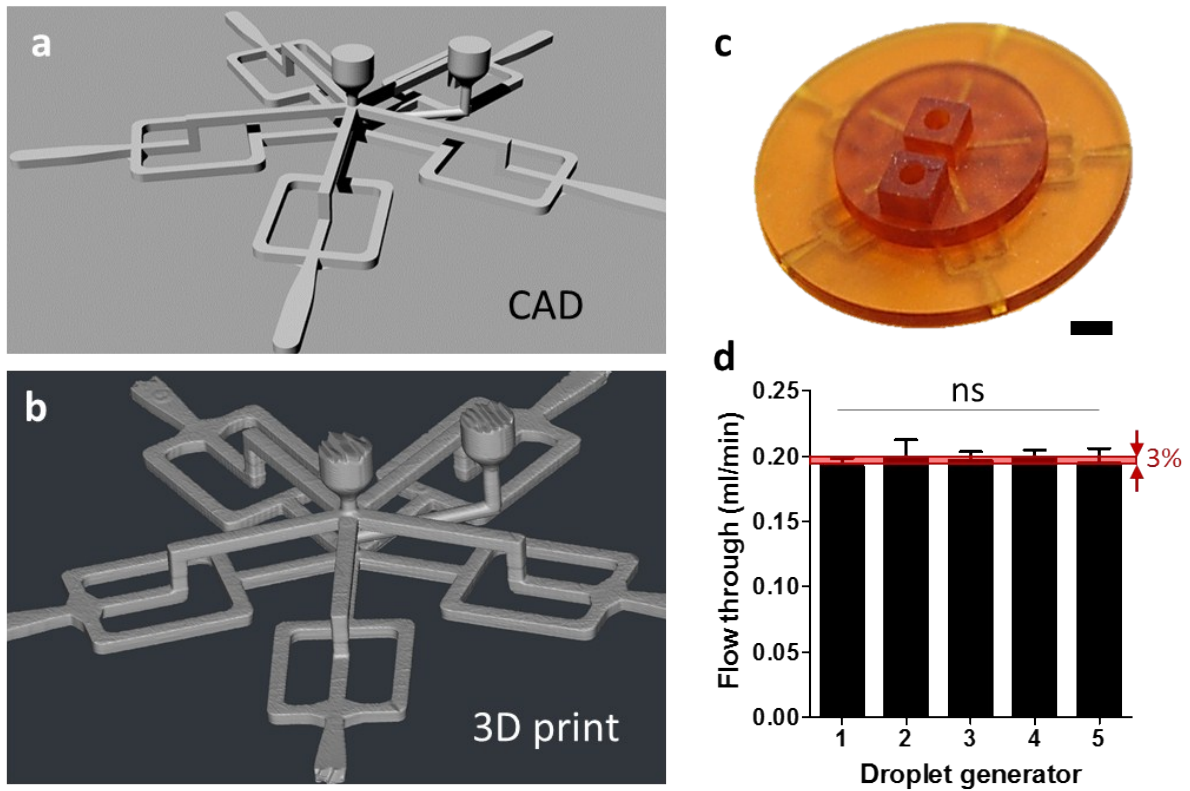
Fig. S6. 3D printed microfluidic device containing parallelized droplet generators using a radial design. (a) A microfluidic device containing five radially placed droplet generators was designed, 3D printed, and (b) analyzed based on 3D reconstructed μCT data to visualize the internal channel structures. (c) Photograph of 3D printed radially parallelized microfluidic device. (d) Flow through (average ± standard deviation; n = 3) of each droplet generator within the radially organized microdevice was quantified and its average fell within the predicted 3% margin. 'ns' indicates p > 0.05; one-way ANOVA. Scale bar indicates 250 μm.

References

1. R. Jin, C. Hiemstra, Z. Zhong and J. Feijen, *Biomaterials*, 2007, **28**, 2791-2800.

2. S. K. Both, A. J. van der Muijsenberg, C. A. van Blitterswijk, J. de Boer and J. D. de Bruijn, *Tissue engineering*, 2007, **13**, 3-9.

3. F. Hecht, *Journal of Numerical Mathematics*, 2012, **20**.

4. T. Kamperman, S. Henke, C. W. Visser, M. Karperien and J. Leijten, *Small*, 2017, DOI: 10.1002/smll.201603711.